Monthly Notices
of the
ROYAL ASTRONOMICAL SOCIETY

MNRAS **466,** 1363–1371 (2017)
Advance Access publication 2016 December 2

doi:10.1093/mnras/stw3125

ExoMol molecular line lists XIX: high-accuracy computed hot line lists for $H_2{}^{18}O$ and $H_2{}^{17}O$

Oleg L. Polyansky,[1,2] Aleksandra A. Kyuberis,[2] Lorenzo Lodi,[1] Jonathan Tennyson,[1]★ Sergei N. Yurchenko,[1] Roman I. Ovsyannikov[2] and Nikolai F. Zobov[2]

[1]*Department of Physics and Astronomy, University College London, London WC1E 6BT, UK*
[2]*Institute of Applied Physics, Russian Academy of Sciences, Ulyanov Street 46, Nizhny Novgorod 603950, Russia*

Accepted 2016 November 29. Received 2016 November 23; in original form 2016 October 20

ABSTRACT

Hot line lists for two isotopologues of water, $H_2{}^{18}O$ and $H_2{}^{17}O$, are presented. The calculations employ newly constructed potential energy surfaces (PES), which take advantage of a novel method for using the large set of experimental energy levels for $H_2{}^{16}O$ to give high-quality predictions for $H_2{}^{18}O$ and $H_2{}^{17}O$. This procedure greatly extends the energy range for which a PES can be accurately determined, allowing an accurate prediction of higher lying energy levels than are currently known from direct laboratory measurements. This PES is combined with a high-accuracy, *ab initio* dipole moment surface of water in the computation of all energy levels, transition frequencies and associated Einstein A coefficients for states with rotational excitation up to $J = 50$ and energies up to 30 000 cm^{-1}. The resulting HotWat78 line lists complement the well-used BT2 $H_2{}^{16}O$ line list. Full line lists are made available online as Supporting Information and at www.exomol.com.

Key words: molecular data – opacity – astronomical data bases: miscellaneous – planets and satellites: atmospheres – brown dwarfs – stars: low-mass.

1 INTRODUCTION

Water spectra can be observed from many different regimes in the Universe, several of which are discussed further below. The spectrum of water, particularly at elevated temperatures, is rich and complex. A few years ago Barber et al. (2006) presented a comprehensive line list, known as BT2, which used well-established theoretical procedures to compute all the transitions of $H_2{}^{16}O$ of importance in objects with temperatures up to 3000 K. BT2 contains about 500 million lines. A similar line list for $HD^{16}O$, known as VTT, was subsequently computed by Voronin et al. (2010).

The BT2 line list has been extensively used. It forms the basis of the most recent release of the HITEMP high-temperature spectroscopic data base (Rothman et al. 2010) and for the BT-Settl model (Allard 2014) for stellar and substellar atmospheres covering the range from solar-mass stars to the latest type T and Y dwarfs. BT2 has been used to detect and analyse water spectra in objects as diverse as the Nova-like object V838 Mon (Banerjee et al. 2005), atmospheres of brown dwarfs (Rice et al. 2010) and M subdwarfs (Rajpurohit et al. 2014), and extensively for exoplanets (Tinetti et al. 2007; Birkby et al. 2013). Within the Solar system BT2 has been used to show an imbalance between nuclear spin and rotational temperatures in cometary comae (Dello Russo et al. 2004, 2005) and assign a new set of, as yet unexplained, high-energy water emissions in comets (Barber et al. 2009), as well as to model water spectra in the deep atmosphere of Venus (Bailey 2009).

Although BT2 was developed for astrophysical use, it has been applied to a variety of other problems including the calculation of the refractive index of humid air in the infrared (Mathar 2007), high-speed thermometry and tomographic imaging in gas engines and burners (Kranendonk et al. 2007; Rein & Sanders 2010), as the basis for an improved theory of line-broadening (Bykov et al. 2008), and to validate the data used in models of the Earth's atmosphere and in particular simulating the contribution of weak water transitions to the so-called water continuum (Chesnokova et al. 2009).

There are several water line lists published in the literature (Partridge & Schwenke 1997; Viti, Tennyson & Polyansky 1997; Mikhailenko, Babikov & Golovko 2005; Barber et al. 2006). Two line lists have also been computed specifically for the isotopologues: Shirin et al. (2008) created the 3mol room-temperature line lists for $H_2{}^{16}O$, $H_2{}^{17}O$ and $H_2{}^{18}O$ based on the potential energy surfaces (PES) of Shirin et al. (2006); Tashkun created a number of line lists based on the work of Partridge & Schwenke (1997) (see Mikhailenko et al. 2005). These are considered further below.

At present, hot line lists are only published for $H_2{}^{16}O$ and $HD^{16}O$. However, isotopically substituted water containing ^{18}O or ^{17}O provides important markers for a variety of astronomical problems (Nittler & Gaidos 2012). For example, Matsuura et al. (2014) recently detected $H_2{}^{18}O$ in the emission-line spectrum of the luminous

★ E-mail: j.tennyson@ucl.ac.uk

Table 1. Comparison of calculated $J = 0$ term values for $H_2{}^{17}O$ using three potentials with experimental data. Experimental (obs.) data are taken from Tennyson et al. (2009).

v_1	v_2	v_3	Observed	PES1	Obs. − Calc.	PES2	Obs. − Calc.	PES3	Obs. − Calc.
0	0	1	3748.318	3748.334	− 0.02	3748.326	− 0.01	3748.463	− 0.15
0	0	2	7431.076	7431.103	− 0.03	7431.059	0.02	7431.467	− 0.39
0	0	3	11 011.883	11 011.936	− 0.05	11 011.860	0.02	11 012.268	− 0.38
0	1	0	1591.326	1591.297	0.03	1591.342	− 0.02	1591.413	− 0.09
0	1	1	5320.251	5320.241	0.01	5320.251	0.00	5320.378	− 0.13
0	1	2	8982.869	8982.868	0.00	8982.844	0.03	8983.118	− 0.25
0	1	3	12 541.227	12 541.267	− 0.04	12 541.207	0.02	12 541.614	− 0.39
0	2	0	3144.980	3144.934	0.05	3144.993	− 0.01	3145.085	− 0.10
0	2	1	6857.273	6857.260	0.01	6857.266	0.01	6857.476	− 0.20
0	7	1	13 808.273	13 808.224	0.05	13 808.371	− 0.10	13 809.171	− 0.90
1	0	0	3653.142	3653.147	0.00	3653.121	0.02	3653.193	− 0.05
1	0	1	7238.714	7238.773	− 0.06	7238.726	− 0.01	7238.932	− 0.22
1	0	2	10 853.505	10 853.545	− 0.04	10 853.504	0.00	–	–
1	0	3	14 296.280	14 296.340	− 0.06	14 296.265	0.01	14 296.584	− 0.30
1	1	0	5227.706	5227.691	0.01	5227.704	0.00	5227.881	− 0.18
1	1	1	8792.544	8792.578	− 0.03	8792.546	0.00	8792.816	− 0.27
1	2	0	6764.726	6764.747	− 0.02	6764.722	0.00	6764.905	− 0.18
1	2	1	10 311.202	10 311.247	− 0.05	10 311.199	0.00	10 311.421	− 0.22
1	3	1	11 792.822	11 792.861	− 0.04	11 792.834	− 0.01	11 793.172	− 0.35
2	0	0	7193.246	7193.265	− 0.02	7193.257	− 0.01	7193.394	− 0.15
2	0	1	10 598.476	10 598.550	− 0.07	10 598.483	− 0.01	10 598.763	− 0.29
2	1	1	12 132.993	12 133.056	− 0.06	12 132.984	0.01	12 132.365	0.63
2	2	1	13 631.500	13 631.542	− 0.04	13 631.489	0.01	13 631.650	− 0.15
3	0	1	13 812.158	13 812.215	− 0.06	13 812.170	− 0.01	13 812.394	− 0.24
3	2	1	16 797.168	16 797.182	− 0.01	16 797.177	− 0.01	16 797.011	0.16
4	0	1	16 875.621	16 875.662	− 0.04	16 875.643	− 0.02	16 875.474	0.15

M-supergiant VY CMa. Astronomical spectra of water isotopologues (Neufeld et al. 2013), and their direct analysis in cometary dust particles (Floss et al. 2010) and carbonaceous chondrites (Clayton & Mayeda 1984; Vollmer, Hoppe & Brenker 2008) have been used to determine formation mechanisms and constrain formation models. Water isotope ratios are also used to monitor stellar evolution (Abia et al. 2012) and to probe the atmosphere of Mars (Villanueva et al. 2015). The seemingly minor isotopologues of water can be important species in their own right with, for example, $H_2{}^{18}O$ being the fifth largest absorber of sunlight in the Earth's atmosphere.

There is therefore a need for line lists equivalent to BT2 for $H_2{}^{17}O$ and $H_2{}^{18}O$ to aid spectroscopic studies, and it is these that are presented here. These lists form part of the ExoMol project (Tennyson & Yurchenko 2012), which aims to provide a comprehensive set of molecular line lists for studies of molecular line lists for exoplanet and other hot atmospheres.

Although our new line lists in some way mimic BT2, they also take advantage of a number of recent theoretical developments. In particular, an IUPAC task group (Tennyson et al. 2014a) used a systematic procedure (Furtenbacher, Császár & Tennyson 2007) to derive empirical energy levels for all the main isotopologues of water (Tennyson et al. 2009, 2010, 2013, 2014b). These levels are combined with a newly developed procedure for enhancing the accuracy of calculations on isotopically substituted species, which is used for the first time here. This ensures that most of the key frequencies in our new line lists are determined with an accuracy close to experimental, even though many of them are yet to be observed. Furthermore, theoretical work on improving the accuracy and representation of the water dipole moment (Lodi et al. 2008; Lodi, Tennyson & Polyansky 2011) has improved the accuracy with which water transition intensities are predicted (Grechko et al. 2009). Some of these advances have already been used to create improved room temperature line lists for $H_2{}^{17}O$ and $H_2{}^{18}O$ (Lodi & Tennyson 2012), which were included in their entirety in the 2012 release of HITRAN (Rothman et al. 2013).

The paper is structured as follows: Section 2 outlines our overall methodology and presents the derivation of PES. The details of the calculation of the new line lists, along with comparison with previous line lists, are given in Section 3. Section 4 discusses further improvement of the line list by the substitution of calculated energy levels with empirical ones, together with the procedure used to label energy levels with approximate vibrational and rotational quantum numbers. Our results are discussed in Section 5.

2 POTENTIAL ENERGY SURFACES

The fitting of water ($H_2{}^{16}O$) PESs to experimental spectroscopic data has a long history. The first fitted PES giving near-to-experimental accuracy was PJT1 (Polyansky, Jensen & Tennyson 1994). Partridge & Schwenke (1997) constructed a fitted PES starting from a highly accurate *ab initio* calculation; all subsequent water potentials followed this procedure and have been based on *ab initio* studies of increasing sophistication. As a result there are several very good water PESs available (Shirin et al. 2003, 2008; Bubukina et al. 2011).

Here we need a PES which satisfies two criteria. First, it should be at least as accurate as the PES used for the BT2 line list with the calculated energies ranging up to 30 000 cm^{-1}. Secondly, the PES should be adapted to the calculation of energy levels of the two water isotopologues $H_2{}^{17}O$ and $H_2{}^{18}O$. This second requirement is harder to fulfill, as the characterization of the experimental energy levels of both $H_2{}^{17}O$ and $H_2{}^{18}O$ is significantly less extensive than for $H_2{}^{16}O$ (Tennyson et al. 2014a).

Table 2. Comparison of calculated $J = 0$ term values for $H_2{}^{18}O$ using three potentials with experimental data. Experimental (obs.) data are taken from Tennyson et al. (2009).

v_1	v_2	v_3	Observed	PES1	Obs. − Calc.	PES2	Obs. − Calc.	PES3	Obs. − Calc.
0	0	1	3741.57	3741.581	− 0.01	3741.567	0.00	3741.575	− 0.01
0	0	2	7418.72	7418.741	− 0.02	7418.693	0.03	7418.759	− 0.03
0	0	3	10 993.68	10 993.734	− 0.05	10 993.659	0.02	10 993.689	− 0.01
0	1	0	1588.28	1588.240	0.04	1588.271	0.00	1588.299	− 0.02
0	1	1	5310.46	5310.443	0.02	5310.438	0.02	5310.388	0.07
0	1	2	8967.57	8967.552	0.01	8967.519	0.05	8967.491	0.07
0	1	3	12 520.12	12 520.153	− 0.03	12 520.089	0.03	12 520.068	0.06
0	2	0	3139.05	3138.999	0.05	3139.038	0.01	3139.031	0.02
0	2	1	6844.60	6844.580	0.02	6844.566	0.03	6844.539	0.06
0	2	2	10 483.22	10 483.264	− 0.04	10 483.202	0.02	10 483.212	0.01
0	3	0	4648.48	4648.435	0.04	4648.469	0.01	4648.452	0.03
0	3	1	8341.11	8341.109	0.00	8341.086	0.02	8341.114	− 0.01
0	3	2	11 963.54	11 963.580	− 0.04	11 963.507	0.03	11 963.615	− 0.08
0	4	0	6110.42	6110.408	0.02	6110.433	− 0.01	6110.410	0.01
0	4	1	9795.33	9795.354	− 0.02	9795.324	0.01	9795.329	0.00
1	0	0	3649.69	3649.688	0.00	3649.649	0.04	3649.667	0.02
1	0	1	7228.88	7228.934	− 0.05	7228.883	0.00	7228.888	0.00
1	0	2	10 839.96	10 839.986	− 0.03	10 839.942	0.01	–	–
1	0	3	14 276.34	14 276.389	− 0.05	14 276.318	0.02	14 276.229	0.11
1	1	0	5221.24	5221.233	0.01	5221.227	0.02	5221.298	− 0.05
1	1	1	8779.72	8779.747	− 0.03	8779.707	0.01	8779.722	0.00
1	1	2	12 372.71	12 372.723	− 0.02	12 372.679	0.03	–	–
1	2	0	6755.51	6755.528	− 0.02	6755.483	0.03	6755.501	0.01
1	2	1	10 295.63	10 295.673	− 0.04	10 295.616	0.02	10 295.524	0.11
1	3	0	8249.04	8249.063	− 0.03	8249.023	0.01	8249.073	− 0.04
1	3	1	11 774.71	11 774.742	− 0.03	11 774.701	0.01	11 774.670	0.04
2	0	0	7185.88	7185.894	− 0.02	7185.879	0.00	7185.880	0.00
2	0	1	10 585.29	10 585.357	− 0.07	10 585.292	− 0.01	10 585.300	− 0.01
2	0	2	14 187.98	14 188.069	− 0.09	14 187.985	0.00	–	–
2	1	0	8739.53	8739.530	0.00	8739.520	0.01	8739.589	− 0.06
2	1	1	12 116.80	12 116.851	− 0.05	12 116.778	0.02	12 116.833	− 0.04
2	2	0	10 256.58	10 256.604	− 0.02	10 256.569	0.02	10 256.537	0.05
2	2	1	13 612.71	13 612.745	− 0.04	13 612.688	0.02	13 612.468	0.24
2	3	0	11 734.53	11 734.543	− 0.02	11 734.517	0.01	11 734.625	− 0.10
3	0	0	10 573.92	10 573.955	− 0.04	10 573.927	− 0.01	10 573.898	0.02
3	0	1	13 795.40	13 795.455	− 0.06	13 795.410	− 0.01	13 795.280	0.12
3	1	0	12 106.98	12 107.025	− 0.05	12 106.974	0.00	12 107.006	− 0.03
3	2	1	16 775.38	16 775.396	− 0.01	16 775.385	0.00	16 774.779	0.60
4	0	1	16 854.99	16 855.126	− 0.14	16 855.099	− 0.11	16 854.534	0.46

To take advantage of the accumulated knowledge on the spectrum $H_2{}^{16}O$ in constructing a PES for $H_2{}^{17}O$ and $H_2{}^{18}O$ and following previous work (Zobov et al. 1996; Voronin et al. 2010; Bubukina et al. 2011), we decided to fit a Born–Oppenheimer (BO) mass-independent PES to the available data for $H_2{}^{16}O$ and fix the adiabatic BO diagonal correction, mass-dependent surface to the *ab initio* value of Polyansky et al. (2003). Obviously, this procedure requires the accuracy of predictions for $H_2{}^{17}O$ and $H_2{}^{18}O$ to be verified. This is done by comparing the calculated $H_2{}^{17}O$ and $H_2{}^{18}O$ energy levels to the available experimentally determined ones (Tennyson et al. 2009, 2010).

We used the same fitting procedure as Bubukina et al. (2011). Nuclear motion calculations were performed with DVR3D (Tennyson et al. 2004). As elsewhere, in the fit the experimentally derived energies of $H_2{}^{16}O$ for the $J = 0$, 2 and 5 rotational states by Tennyson et al. (2013) were used.

In the following, our new empirical PES obtained using the fitting procedure described above will be referenced to as PES1, while the PES by Bubukina et al. (2011) will be referenced to as PES2. Tables 1 and 2 present a comparison between the $J = 0$ energy levels calculated using PES1, PES2 for $H_2{}^{17}O$ and $H_2{}^{18}O$, respectively. For comparison as a third column, we present the $J = 0$ levels and corresponding discrepancies using the PES (called PES3 in the tables) due to Partridge & Schwenke (1997) taken from the line list calculated by Dr S. A. Tashkun and summarized by Mikhailenko et al. (2005). The line list based on PES3 was calculated for three temperatures: $T = 296$, 1000 and 3000 K. For all versions, the highest value of the rotational quantum number J considered is 28 and the spectral range is 0–28500 cm^{-1}. The number of lines for $H_2{}^{18}O$ is 108 784 and for $H_2{}^{17}O$ is 109 083.

Indeed, one can see that the agreement with the experiment is very good. Although the results obtained using PES2 are somewhat better than those for PES1. However, employing PES1 gives us the opportunity to use the information on $H_2{}^{16}O$ experimental energy levels to predict very accurately energy levels of $H_2{}^{17}O$ and $H_2{}^{18}O$. We call these predicted levels pseudo-experimental energies for the reasons explained below. Table 3 illustrates the unprecedented accuracy of the prediction of the $H_2{}^{17}O$ energy levels for those states whose energies are known experimentally. The slightly less good, but still very accurate, energy levels predicted for $H_2{}^{18}O$ are

Table 3. Standard deviation in cm^{-1} with which our pseudo-experimental energy levels of $H_2{}^{17}O$ and $H_2{}^{18}O$ predict the observed ones compiled by Tennyson et al. (2010) as a function of rotational state, J, N is number of levels used for calculation of the standard deviation.

J	N	$H_2{}^{17}O$	N	$H_2{}^{18}O$
0	27	0.0058	39	0.0092
1	93	0.0056	124	0.0093
2	161	0.0071	212	0.0109
3	199	0.0074	254	0.0090
4	236	0.0118	316	0.0147
5	232	0.0103	335	0.0141
6	263	0.0100	401	0.0116
7	222	0.0138	385	0.0140
8	182	0.0146	381	0.0130
9	138	0.0123	335	0.0174
10	116	0.0130	288	0.0176
11	72	0.0080	232	0.0168
12	47	0.0111	188	0.0201
13	26	0.0083	135	0.0179
14	9	0.0096	106	0.0198
15	3	0.0150	73	0.0176
16	1	0.0066	46	0.0184
17	1	0.0015	19	0.0156
18			11	0.0187

Table 4. Prediction of experimental energy levels of $H_2{}^{18}O$. Experimental (obs.) data are taken from Makarov et al. (2015).

J	Observed	Calculated	Obs. − Calc.
0	27 476.33	27 476.24	0.09
1	27 497.03	27 496.92	0.11
1	27 510.64	27 510.31	0.33
1	27 517.09	27 517.44	−0.35
2	27 537.12	27 536.96	0.16
2	27 546.82	27 546.45	0.37
1	27 509.55	27 509.19	0.36
2	27 545.66	27 545.28	0.38

shown in the column 2 of Table 3. We might expect a similar level of accuracy for predictions of the $H_2{}^{17}O$ and $H_2{}^{18}O$ energy levels for states yet to be measured for these isotopologues, but known for $H_2{}^{16}O$. We note that the standard deviations given in Table 3 are rather systematic suggesting that further improvement in the predictions may be possible. This and details of our final pseudo-experimental energy levels are discussed in Section 4.

Recently, high-lying energy levels of $H_2{}^{18}O$ have been measured using multiphoton spectroscopy (Makarov et al. 2015). These levels lie at about 27 000 cm^{-1} and therefore provide a stringent test of our procedure. The highest upper energy level considered in this work, as for BT2, is 30 000 cm^{-1}; Table 4 illustrates the high quality of our calculations over the whole range considered. In fact, recent studies confirm that BT2 is not so accurate for these high energy states (Lampel et al. 2017).

Thus, the line lists, details of whose calculations are given in the following section, are computed using a higher quality PES than that used to compute BT2. Three sets of energy levels are provided as part of this line list. The first set is the variationally calculated energy levels obtained using PES2. The second set comprises these energy levels substituted by the experimental values (Tennyson et al. 2009) where available. The third set comprises pseudo-experimental energy levels substituted whenever $H_2{}^{16}O$ experimental energy levels (Tennyson et al. 2013) are available (see below). This third set is the one we recommend for creating spectra with HotWat78 because of its increased accuracy.

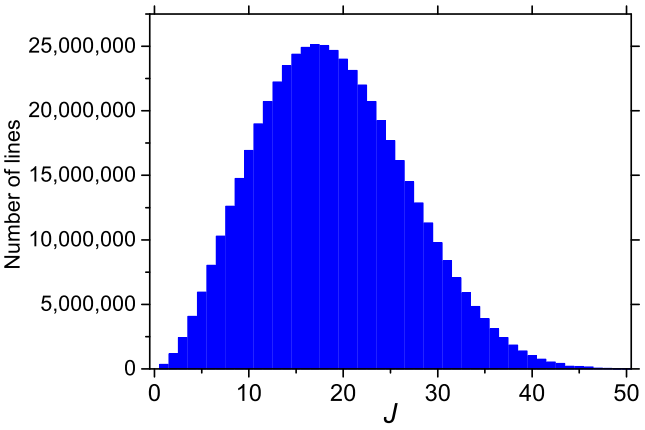

Figure 1. The distribution of the $H_2{}^{18}O$ transitions per J in the line HotWat78 list.

3 LINE-LIST CALCULATIONS FOR $H_2{}^{17}O$ AND $H_2{}^{18}O$

The line-list calculations were performed with the DVR3D program suite (Tennyson et al. 2004) using the PES1 and PES2 discussed above and the *ab initio* dipole moment surface LTP2011S of Lodi et al. (2011). As for BT2, the highest rotational state, J, in the calculation was taken as $J = 50$ and the limiting energy as 30 000 cm^{-1}. Analysis using the $H_2{}^{16}O$ partition function (Vidler & Tennyson 2000) performed in BT2 suggests that these parameters are sufficient to cover all transitions longwards of 0.5 μm for temperatures up to 3000 K.

Wavefunctions were obtained by solving the nuclear-motion Schrödinger equation using a two-step procedure of calculation for the rovibrational energies (Tennyson & Sutcliffe 1986). The calculations benefitted from recent algorithmic improvements (Tennyson & Yurchenko 2017), in particular in the method used to construct the final Hamiltonian matrices for $J > 0$ due to Azzam et al. (2016). Transition intensities were computed for $\Delta J = 0$ and 1 for all four symmetries and every $J \leq 50$. The matrix elements of the dipole moment surface (DMS) were calculated using the program DIPOLE of the suite DVR3D, and the actual spectrum for both isotopologues was generated with the program SPECTRA. About 500 million transitions were calculated for each isotopologue.

Fig. 1 shows the distribution of the $H_2{}^{18}O$ lines in HotWat78.

Using our calculations, we provide the values of partition function for both isotopologues for wide range of temperatures, which are presented in the Table 5 as well as in the supplementary data on a grid of 1 K. We use the HITRAN convention (Fischer et al. 2003) and include the nuclear statistical weights g_{ns} into the partition function explicitly (Tennyson et al. 2016). The nuclear statistical weights for $H_2{}^{18}O$ are the same as for the main isotopologue, 1 and 3 for the para and ortho states, respectively. In case of $H_2{}^{17}O$, g_{ns} are 6 (para) and 18 (ortho). For the calculation of partition functions for $H_2{}^{18}O$ and $H_2{}^{17}O$, we used all available energy levels by applying the cut-off at 30 000 cm^{-1}.

Table 5. Partition functions of $H_2{}^{17}O$ and $H_2{}^{18}O$.

T(K)	$H_2{}^{17}O$	$H_2{}^{18}O$
10	7.979 708 59	1.331 350 07
20	20.162 9004	3.370 744 65
40	56.729 2812	9.488 606 74
60	101.331 587	16.950 9639
80	153.237 432	25.635 7152
100	211.822 453	35.438 2143
200	587.053 283	98.223 7727
296	1052.122 02	176.043 783
300	1073.453 56	179.613 285
400	1654.786 25	276.895 547
500	2328.515 05	389.655 412
600	3099.262 94	518.674 912
800	4966.658 92	831.352 302
1000	7346.851 87	1230.028 25
1200	10 357.5304	1734.467 24
1400	14 140.2160	2368.432 92
1500	16 371.1820	2742.404 04
1600	18 857.9004	3159.293 45
1800	24 694.5428	4137.938 95
2000	31 855.8230	5338.909 08
2200	40 570.4778	6800.617 46
2400	51 091.7815	8565.599 49
2500	57 116.1119	9576.292 00
2600	63 698.8388	10 680.7274
2800	78 697.3411	13 197.3344
3000	96 419.4218	16 171.1873
3200	117 222.299	19 662.2543
3400	141 485.523	23 734.2409
3500	155 038.487	26 008.8411
3600	169 606.832	28 453.8904
3800	201 996.792	33 890.0829
4000	239 072.534	40 112.7834
4200	281 250.969	47 191.9028
4400	328 941.890	55 196.1417
4500	354 979.000	59 566.0429
4600	382 541.321	64 191.8753
4800	442 425.403	74 242.1299
5000	508 945.054	85 405.6885
5200	582 421.516	97 736.3470
5400	663 142.877	111 282.333
5500	706 300.716	118 524.515
5600	751 361.549	126 085.883
5800	847 292.676	148 990.861
6000	951 113.377	159 603.233

4 IMPROVED PSEUDO-EXPERIMENTAL ENERGY LEVELS

The series of IUPAC papers on the various isotopologues of water (Tennyson et al. 2009, 2010, 2013, 2014b) used measured transition frequencies to derive rovibrational energy levels using the so-called MARVEL (measured active rotation–vibration energy levels) procedure (Furtenbacher et al. 2007; Furtenbacher & Császár 2012). These energy levels can be used to generate pseudo-experimental values of the line frequencies in our line lists when the calculated energy level is substituted by the corresponding (pseudo-)experimental one. The comparison of these generated line frequencies with actual experimental ones demonstrate near-perfect coincidence. The number of generated pseudo-experimental lines is significantly higher than the number of the directly observed lines because line frequencies between pseudo-experimental levels can be predicted to high accuracy even when the lines have not been measured, as demonstrated by Tennyson et al. (2013). Less than 200 000 experimentally observed $H_2{}^{16}O$ lines give rise to about 5000 000 lines with pseudo-experimental frequencies generated in this way. Use of such a procedure provides significantly more accurate line lists than just the calculated ones. We therefore substituted our computed energy with those of Tennyson et al. (2009) wherever possible.

However, as described in Section 2, the procedure for fitting PES using $H_2{}^{16}O$ data opens the way for us to further improve the accuracy of the calculated line lists. Looking at Table 6, we can see that the obs. − calc. residuals for a particular $H_2{}^{16}O$ vibrational state are very similar to the residuals for the same states of $H_2{}^{17}O$ and $H_2{}^{18}O$. The following procedure can be used to exploit this. First, let us consider the idealized situation when all the residuals for energy levels of $H_2{}^{16}O$, $R_{v,J}(16)$, are exactly equal to those of $H_2{}^{18}O$, $R_{v,J}(18)$, where (v, J) represent the vibrational and rotational quantum numbers. In this case, we can predict the precise 'estimated' value of an $H_2{}^{18}O$ level, $E^{\rm est}_{v,J}(18)$, from the empirically determined levels of $H_2{}^{16}O$, $E^{\rm obs}_{v,J}(18)$:

$$E^{\rm est}_{v,j}(18) = E^{\rm calc}_{v,J}(18) + R_{v,J}(18) = E^{\rm calc}_{v,J}(18) + R_{v,J}(16), \quad (1)$$

where $E^{\rm calc}_{v,J}(18)$ is the corresponding calculated $H_2{}^{18}O$ energy level. So even if the level of the $H_2{}^{18}O$ isotopologue has yet to be observed, its pseudo-experimental value can be retrieved from the calculated level of $H_2{}^{18}O$ using our calculations plus the residual for $H_2{}^{16}O$, provided the experimental level of $H_2{}^{16}O$ is known.

Table 6 shows that residuals for $H_2{}^{16}O$ and $H_2{}^{18}O$ are slightly different; we can therefore improve this procedure. We notice from Table 6 that the $H_2{}^{16}O$ and $H_2{}^{18}O$ residuals differ by similar amounts. If we average this value, we get

$$\Delta R(18) = \frac{1}{N}\sum_{v=1}^{N} R_{v,0}(18) - R_{v,0}(16), \quad (2)$$

where N runs over the number of vibrational states for which $J = 0$ levels are known, which corresponds to 40 for $H_2{}^{17}O$ and 24 for $H_2{}^{18}O$. Then we can use this average difference to further correct our estimated $H_2{}^{18}O$ energy levels using the revised formula

$$E^{\rm est}_{v,j}(18) = E^{\rm calc}_{v,J}(18) + R_{v,J}(16) + \Delta R(18). \quad (3)$$

Calculating the observed values of energies of $H_2{}^{18}O$ using equation (1) gives a standard deviation for $E^{\rm est}_{v,j}(18)$ levels from the known experimental values, $E^{\rm obs}_{v,j}(18)$, of 0.009 $\rm cm^{-1}$. However, $\Delta R(18)$ is 0.006 $\rm cm^{-1}$. If instead we use equation (3), then the standard deviation reduces to 0.003 $\rm cm^{-1}$. Although $\Delta R(18)$ is evaluated for $J = 0$ only, this procedure still works for higher J values. For example, it also results in a standard deviation of 0.003 $\rm cm^{-1}$ when applied to the $J = 10$ levels of the (010) state.

This procedure, which can clearly also be applied to $H_2{}^{17}O$, leads to the generation of about five million transitions, which involve the pseudo-experimental levels of $H_2{}^{17}O$ and $H_2{}^{18}O$. It therefore provides a line list with much more accurate values of the frequencies of these transitions: in general, better by about 0.005 $\rm cm^{-1}$ for $H_2{}^{17}O$ and somewhat worse for $H_2{}^{18}O$, but still much more accurate than possible with variational calculations.

The reason this procedure can be applied to the construction of the pseudo-experimental values of the energy levels of minor isotopologues is that for the major water isotopologue $H_2{}^{16}O$, the number of energy levels known experimentally is significantly higher than that for $H_2{}^{17}O$ and $H_2{}^{18}O$. For example, the assignment of weak $H_2{}^{16}O$ lines in various regions is available (Polyansky et al. 1998; Schermaul et al. 2002; Tolchenov et al. 2005), where isotopologues data are not known. As a result very highly excited bending (Polyansky et al. 1997; Zobov et al. 2005) and

Table 6. Vibrational band origins, in cm^{-1}, for $H_2{}^{16}O$, $H_2{}^{17}O$ and $H_2{}^{18}O$. Observed (obs.) data are taken from Tennyson et al. (2009, 2013); calculated results are given as observed minus calculated (o − c).

$(v_1v_2v_3)$	$H_2{}^{16}O$ Obs.	O − C	$H_2{}^{17}O$ Obs.	O − C	$H_2{}^{18}O$ Obs.	O − C
(010)	1594.75	0.019	1591.33	0.028	1588.28	0.036
(020)	3151.63	0.040	3144.98	0.046	3139.05	0.051
(100)	3657.05	−0.007	3653.14	−0.005	3649.69	−0.002
(110)	5234.97	0.005	5227.71	0.014	5221.24	0.010
(120)	6775.09	−0.028	6764.73	−0.022	6755.51	−0.018
(200)	7201.54	−0.024	7193.25	−0.019	7185.88	−0.016
(012)	9000.14	−0.009	8982.87	0.001	8967.57	0.013
(102)	10 868.88	−0.049	10 853.51	−0.040	10 839.96	−0.030
(001)	3755.93	−0.017	3748.32	−0.015	3741.57	−0.014
(011)	5331.27	−0.002	5320.25	0.010	5310.46	0.019
(021)	6871.52	0.004	6857.27	0.012	6844.60	0.019
(101)	7249.82	−0.063	7238.71	−0.059	7228.88	−0.051
(111)	8807.00	−0.044	8792.54	−0.034	8779.72	−0.027
(121)	10 328.73	−0.055	10 311.20	−0.045	10 295.63	−0.039
(201)	10 613.36	−0.074	10 598.48	−0.075	10 585.29	−0.072
(003)	11 032.40	−0.061	11 011.88	−0.053	10 993.68	−0.053
(131)	11 813.20	−0.041	11 792.82	−0.039	11 774.71	−0.034
(211)	12 151.25	−0.072	12 132.99	−0.064	12 116.80	−0.054
(113)	12 565.01	−0.050	12 541.23	−0.041	12 520.12	−0.030
(221)	13 652.66	−0.045	13 631.50	−0.042	13 612.71	−0.035
(301)	13 830.94	−0.062	13 812.16	−0.057	13 795.40	−0.057
(103)	14 318.81	−0.069	14 296.28	−0.061	14 276.34	−0.053

Table 7. Extract from the final states file for $H_2{}^{17}O$.

i	$\tilde{E}$	g_{tot}	J	K_a	K_c	v_1	v_2	v_3	S
1	0.000 000	6	0	0	0	0	0	0	A1
2	1591.322 876	6	0	0	0	0	1	0	A1
3	3144.980 225	6	0	0	0	0	2	0	A1
4	3653.145 752	6	0	0	0	1	0	0	A1
5	4657.115 211	6	0	0	0	0	3	0	A1
6	5227.703 125	6	0	0	0	1	1	0	A1
7	6121.557 129	6	0	0	0	0	4	0	A1
8	6764.726 562	6	0	0	0	1	2	0	A1
9	7193.246 582	6	0	0	0	2	0	0	A1
10	7431.093 262	6	0	0	0	0	0	2	A1
11	7527.489 258	6	0	0	0	0	5	0	A1
12	8260.781 250	6	0	0	0	1	3	0	A1
13	8749.905 273	6	0	0	0	2	1	0	A1
14	8853.288 086	6	0	0	0	0	6	0	A1
15	8982.860 352	6	0	0	0	0	1	2	A1
16	9708.538 086	6	0	0	0	1	4	0	A1
17	10 068.091 797	6	0	0	0	0	7	0	A1
18	10 269.661 133	6	0	0	0	2	2	0	A1
19	10 501.353 516	6	0	0	0	0	2	2	A1
20	10 586.049 805	6	0	0	0	3	0	0	A1

Notes. i: state counting number; $\tilde{E}$: state energy in cm^{-1}; g_{tot}: total state degeneracy. J: total angular momentum; K_a: asymmetric top quantum number; K_c: asymmetric top quantum number; v_1: symmetric stretch quantum number; v_2: bending quantum number; v_3: asymmetric stretch quantum number; S: state symmetry in C_{2v}.

Table 8. Extract from the transitions file for $H_2{}^{17}O$.

f	i	A_{fi}
142 344	150 189	5.6651e−05
2235	2362	1.7434e−03
34 497	35 342	5.7700e−09
125 681	114 596	5.5394e−10
135 143	128 340	6.3329e−08
24 055	16 736	1.5208e−03
147 918	137 719	1.3405e−04
45 027	45 537	8.0306e−07
37 457	31 884	9.0168e−08
39 192	43 632	7.3676e−07
25 153	26 085	4.3393e−05
131 146	124 272	8.5679e−04
134 840	128 287	8.5680e−04
88 744	94 220	1.2221e−03
102 017	106 580	2.4131e−04
193 489	187 074	2.7697e−06
202 910	204 558	7.0571e−03
53 725	50 906	1.8345e−06
142 862	135 857	2.5908e−05

Notes. f: upper state counting number; i: lower state counting number; A_{fi}: Einstein-A coefficient in s^{-1}.

stretching energy levels (Maksyutenko et al. 2007; Grechko et al. 2009; Császár et al. 2010) are known, which form the basis upon which our pseudo-experimental energy levels are constructed.

5 RESULTS

The newly constructed $H_2{}^{17}O$ and $H_2{}^{18}O$ line lists are named HotWat78. The new HotWat78 line lists are calculated for $J \leq 50$ and for the spectral range 0–30 000 cm^{-1}. HotWat78 contains 519 461 789 lines for $H_2{}^{18}O$ and 513 062 380 lines for $H_2{}^{17}O$. The new line lists are both the most complete and the most accurate one, see Tables 1 and 2. They are stored in the ExoMol format (Tennyson, Hill & Yurchenko 2013), which uses the compact storage of results originally developed for BT2. This involves using a states file (`.states`), see Table 7, and a transitions file (`.trans`), see Table 8. The energy levels in the states files are marked as 'observed' if the results are taken from the IUPAC compilation, 'estimated' if

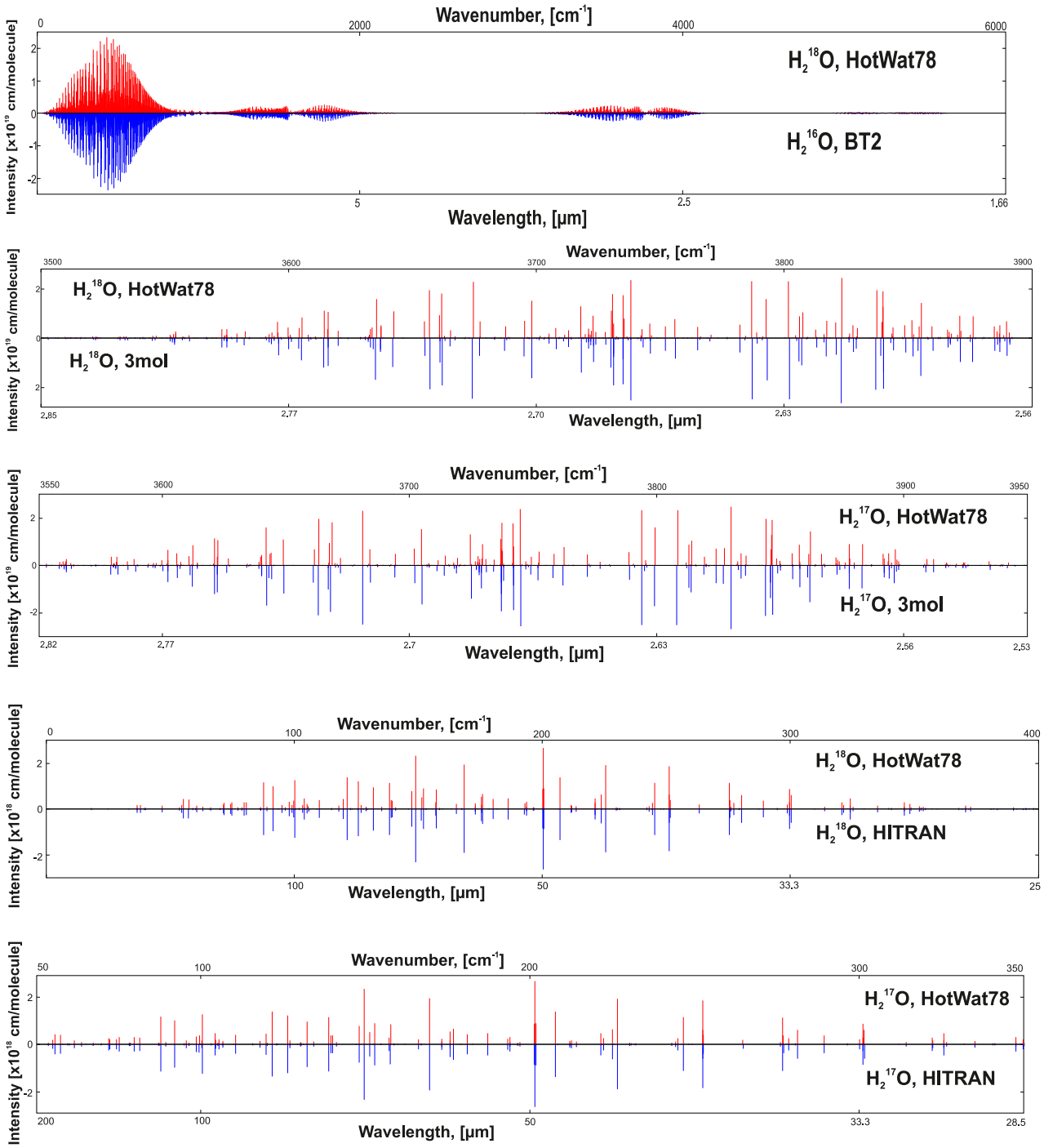

Figure 2. Comparison between BT2 and HotWat78 for $H_2{}^{18}O$ at the temperature $T = 2000$ K, and comparison of HotWat78 with 3mol (Shirin et al. 2008) and HITRAN at $T = 296$ K for $H_2{}^{18}O$ and $H_2{}^{17}O$, respectively.

they are generated using equation (3) or as 'calculated', for which the results of the PES2 calculation are used.

The states file lists all the rovibrational levels for each J and for four C_{2v} symmetries. It is common to further label every level with (approximate) vibrational quantum numbers (v_1, v_2, v_3), which correspond to the symmetric stretch, bending and asymmetric stretch modes, respectively, and the rotational levels within each vibrational state by J, K_a and K_c, where again the projection quantum numbers K_a and K_c are approximate. DVR3D does not provide these approximate labels but there are several methods available for labelling water energy levels (Partridge & Schwenke 1997; Szidarovszky, Fabri & Császár 2012; Shirin et al. 2008). Here we label levels with $J \leq 20$ and energies below 20 000 cm^{-1}. As our energy levels differ by less than 1 cm^{-1} from those of Shirin et al. (2008), transferring the labels from this previous study proved to be straightforward. We note that the labels we use are based on the normal modes from a harmonic oscillator model. It is well know that the higher stretching states of water are better represented with

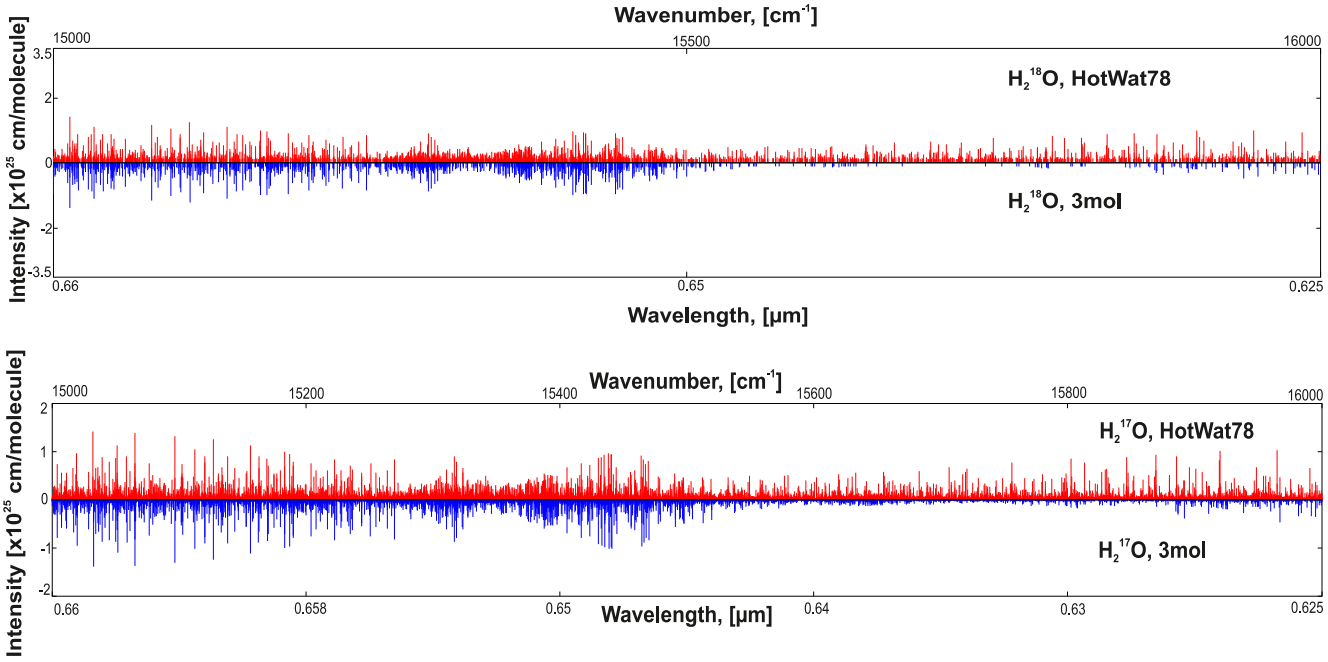

Figure 3. Comparison of $H_2{}^{18}O$ and $H_2{}^{17}O$ between 3mol (Shirin et al. 2008) and HotWat78 at the temperature $T = 3000$ K.

a local-mode model (Child & Halonen 1984). However, there is a one-to-one correspondence between the two labelling schemes (Carleer et al. 1999); the use of normal-mode labels are used for simplicity.

The accuracy of the present line lists can be established by the comparison with the previous line-list calculations. Two types of comparison could be made. The overall picture for the high temperature is that the coverage of the HotWat78 $H_2{}^{17}O$ and $H_2{}^{18}O$ line lists should be very similar to BT2, but that both the predicted intensives and the line positions should be significantly better. Furthermore, lines may shift by a few cm^{-1} to a few tens of cm^{-1} between isotopologues. Fig. 1 demonstrates that, as expected, the overall picture is very similar for BT2 ($H_2{}^{16}O$) and HotWat78 ($H_2{}^{17}O$ and $H_2{}^{18}O$). Here we provide the comparison only for $H_2{}^{18}O$ but the comparison for $H_2{}^{17}O$ looks the same.

Figs 2 and 3 illustrate the similarity of the HotWat78 line lists with the previous high-accuracy $H_2{}^{17}O$ and $H_2{}^{18}O$ line lists (called 3mol) of Shirin et al. (2008) for these molecules at the room temperature. Fig. 2 also provides a comparison with the HITRAN data for the room temperature for $H_2{}^{17}O$ and $H_2{}^{18}O$. These figures only provide an overview, but a detailed line by line comparison confirms that all the calculations we present here are done correctly.

The present line lists are significantly more complete, but this is only apparent at higher temperatures (see Fig. 3). For the room temperature, the previous line lists should look similar, as they indeed do (see Fig. 2).

6 CONCLUSIONS

This paper reports hot line lists for $H_2{}^{17}O$ and $H_2{}^{18}O$. These line lists represent significant improvement on both coverage and accuracy of the previous $H_2{}^{17}O$ and $H_2{}^{18}O$ line lists (Mikhailenko et al. 2005; Shirin et al. 2008). The predicted frequencies in these line lists are significantly improved using information obtained from the corresponding $H_2{}^{16}O$ empirical energy levels. This procedure can be adapted to give improved predictions of energy levels and transition frequencies for isotopologues of molecules for whom the empirical energy levels of the parent molecule are well known.

The complete HotWat78 line lists for $H_2{}^{17}O$ and $H_2{}^{18}O$ can be downloaded from the CDS, via ftp://cdsarc.u-strasbg.fr/pub/cats/J/MNRAS/ or via http://cdsarc.u-strasbg.fr/viz-bin/qcat?J/MNRAS/. The line lists together with auxiliary data including the potential parameters, dipole moment functions and theoretical energy levels can be also obtained at www.exomol.com, where they form part of the enhanced ExoMol data base (Tennyson et al. 2016). The BT2 $H_2{}^{16}O$ line list (Barber et al. 2006) is already available from these sources.

Finally, we note that pressure-broadening has been shown to have a significant effect on water spectra in exoplanets (Tinetti et al. 2012). ExoMol, in common with other data bases, assumes that pressure-broadening parameters for $H_2{}^{17}O$ and $H_2{}^{18}O$ are the same as those for $H_2{}^{16}O$. This assumption is built into the recently updated structure of the ExoMol data base (Tennyson et al. 2016). Barton et al. (2017a) have recently presented a comprehensive set of pressure-broadening parameters for $H_2{}^{16}O$ lines that form the basis for the ExoMol pressure-broadening diet for water (Barton et al. 2017b). These parameters, which are available on the ExoMol web site, are also suitable for use with the HotWat78 line lists.

ACKNOWLEDGEMENTS

This work is supported by ERC Advanced Investigator Project 267219 and by the Russian Foundation for Basic Research.

REFERENCES

Abia C., Palmerini S., Busso M., Cristallo S., 2012, A&A, 548, A55
Allard F., 2014, in Booth M., Matthews B. C., Graham J. R., eds, Proc. IAU Symp. 299, Exploring the Formation and Evolution of Planetary Systems. Cambridge Univ. Press, Cambridge, p. 271

Azzam A. A. A., Yurchenko S. N., Tennyson J., Naumenko O. V., 2016, MNRAS, 460, 4063
Bailey J., 2009, Icarus, 201, 444
Banerjee D. P. K., Barber R. J., Ashok N. K., Tennyson J., 2005, ApJ, 627, L141
Barber R. J., Tennyson J., Harris G. J., Tolchenov R. N., 2006, MNRAS, 368, 1087
Barber R. J., Miller S., Dello Russo N., Mumma M. J., Tennyson J., Guio P., 2009, MNRAS, 398, 1593
Barton E. J., Hill C., Yurchenko S. N., Tennyson J., Dudaryonok A., Lavrentieva N. N., 2017a, J. Quant. Spectrosc. Radiat. Transfer, 187, 453
Barton E. J., Hill C., Czurylo M., Li H.-Y., Hyslop A., Yurchenko S. N., Tennyson J., 2017b, J. Quant. Spectrosc. Radiat. Transfer, in press
Birkby J. L., de Kok R. J., Brogi M., de Mooij E. J. W., Schwarz H., Albrecht S., Snellen I. A. G., 2013, MNRAS, 436, L35
Bubukina I. I., Polyansky O. L., Zobov N. F., Yurchenko S. N., 2011, Opt. Spectrosc., 110, 160
Bykov A. D., Lavrientieva N. N., Mishina T. P., Sinitsa L. N., Barber R. J., Tolchenov R. N., Tennyson J., 2008, J. Quant. Spectrosc. Radiat. Transfer, 109, 1834
Carleer M. et al., 1999, J. Chem. Phys., 111, 2444
Chesnokova T. Y., Voronin B. A., Bykov A. D., Zhuravleva T. B., Kozodoev A. V., Lugovskoy A. A., Tennyson J., 2009, J. Mol. Spectrosc., 256, 41
Child M. S., Halonen L., 1984, Adv. Chem. Phys., 57, 1
Clayton R. N., Mayeda T. K., 1984, Earth Planet. Sci. Lett., 67, 151
Császár A. G., Mátyus E., Lodi L., Zobov N. F., Shirin S. V., Polyansky O. L., Tennyson J., 2010, J. Quant. Spectrosc. Radiat. Transfer, 111, 1043
Dello Russo N., DiSanti M. A., Magee-Sauer K., Gibb E. L., Mumma M. J., Barber R. J., Tennyson J., 2004, Icarus, 168, 186
Dello Russo N., Bonev B. P., DiSanti M. A., Gibb E. L., Mumma M. J., Magee-Sauer K., Barber R. J., Tennyson J., 2005, ApJ, 621, 537
Fischer J., Gamache R. R., Goldman A., Rothman L. S., Perrin A., 2003, J. Quant. Spectrosc. Radiat. Transfer, 82, 401
Floss C., Stadermann F. J., Mertz A. F., Bernatowicz T. J., 2010, Meteorit. Planet. Sci., 45, 1889
Furtenbacher T., Császár A. G., 2012, J. Quant. Spectrosc. Radiat. Transfer, 113, 929
Furtenbacher T., Császár A. G., Tennyson J., 2007, J. Mol. Spectrosc., 245, 115
Grechko M. et al., 2009, J. Chem. Phys., 131, 221105
Kranendonk L. A. et al., 2007, Opt. Express, 15, 15115
Lampel J. et al., 2017, Atmos. Chem. Phys., in press
Lodi L., Tennyson J., 2012, J. Quant. Spectrosc. Radiat. Transfer, 113, 850
Lodi L. et al., 2008, J. Chem. Phys., 128, 044304
Lodi L., Tennyson J., Polyansky O. L., 2011, J. Chem. Phys., 135, 034113
Makarov D. S., Koshelev M. A., Zobov N. F., Boyarkin O. V., 2015, Chem. Phys. Lett., 627, 73
Maksyutenko P., Muenter J. S., Zobov N. F., Shirin S. V., Polyansky O. L., Rizzo T. R., Boyarkin O. V., 2007, J. Chem. Phys., 126, 241101
Mathar R. J., 2007, J. Optics, 9, 470
Matsuura M. et al., 2014, MNRAS, 437, 532
Mikhailenko S. N., Babikov Y. L., Golovko V. F., 2005, Atmos. Ocean. Opt., 18, 685
Neufeld D. A. et al., 2013, ApJ, 767, L3
Nittler L. R., Gaidos E., 2012, Meteorit. Planet. Sci., 47, 2031
Partridge H., Schwenke D. W., 1997, J. Chem. Phys., 106, 4618
Polyansky O. L., Jensen P., Tennyson J., 1994, J. Chem. Phys., 101, 7651
Polyansky O. L., Zobov N. F., Tennyson J., Lotoski J. A., Bernath P. F., 1997, J. Mol. Spectrosc., 184, 35
Polyansky O. L., Zobov N. F., Viti S., Tennyson J., 1998, J. Mol. Spectrosc., 189, 291
Polyansky O. L., Császár A. G., Shirin S. V., Zobov N. F., Barletta P., Tennyson J., Schwenke D. W., Knowles P. J., 2003, Science, 299, 539
Rajpurohit A. S., Reyle C., Allard F., Scholz R. D., Homeier D., Schultheis M., Bayo A., 2014, A&A, 564, A90
Rein K. D., Sanders S. T., 2010, Appl. Opti., 49, 4728
Rice E. L., Barman T., Mclean I. S., Prato L., Kirkpatrick J. D., 2010, ApJS, 186, 63
Rothman L. S. et al., 2010, J. Quant. Spectrosc. Radiat. Transfer, 111, 2139
Rothman L. S. et al., 2013, J. Quant. Spectrosc. Radiat. Transfer, 130, 4
Schermaul R., Learner R. C. M., Canas A. A. D., Brault J. W., Polyansky O. L., Belmiloud D., Zobov N. F., Tennyson J., 2002, J. Mol. Spectrosc., 211, 169
Shirin S. V., Polyansky O. L., Zobov N. F., Barletta P., Tennyson J., 2003, J. Chem. Phys., 118, 2124
Shirin S. V., Polyansky O. L., Zobov N. F., Ovsyannikov R. I., Császár A. G., Tennyson J., 2006, J. Mol. Spectrosc., 236, 216
Shirin S. V., Zobov N. F., Ovsyannikov R. I., Polyansky O. L., Tennyson J., 2008, J. Chem. Phys., 128, 224306
Szidarovszky T., Fabri C., Császár A. G., 2012, J. Chem. Phys., 136, 174112
Tennyson J., Sutcliffe B. T., 1986, Mol. Phys., 58, 1067
Tennyson J., Yurchenko S. N., 2012, MNRAS, 425, 21
Tennyson J., Yurchenko S. N., 2017, Int. J. Quantum Chem., 117, 92
Tennyson J., Kostin M. A., Barletta P., Harris G. J., Polyansky O. L., Ramanlal J., Zobov N. F., 2004, Comput. Phys. Commun., 163, 85
Tennyson J. et al., 2009, J. Quant. Spectrosc. Radiat. Transfer, 110, 573
Tennyson J. et al., 2010, J. Quant. Spectrosc. Radiat. Transfer, 111, 2160
Tennyson J. et al., 2013, J. Quant. Spectrosc. Radiat. Transfer, 117, 29
Tennyson J., Hill C., Yurchenko S. N., 2013, in Gillaspy J. D., Wiese W. L., Podpaly Y. L., eds, AIP Conf. Proc. Vol. 1545, Data Structures for ExoMol: Molecular Line Lists for Exoplanet and Other Atmospheres. The Sun. Am. Inst. Phys., New York, p. 186
Tennyson J. et al., 2014a, Pure Appl. Chem., 86, 71
Tennyson J. et al., 2014b, J. Quant. Spectrosc. Radiat. Transfer, 142, 93
Tennyson J. et al., 2016, J. Mol. Spectrosc., 327, 73
Tinetti G. et al., 2007, Nature, 448, 169
Tinetti G., Tennyson J., Griffiths C. A., Waldmann I., 2012, Phil. Trans. R. Soc. A, 370, 2749
Tolchenov R. N. et al., 2005, J. Mol. Spectrosc., 233, 68
Vidler M., Tennyson J., 2000, J. Chem. Phys., 113, 9766
Villanueva G. L. et al., 2015, Science, 348, 218
Viti S., Tennyson J., Polyansky O. L., 1997, MNRAS, 287, 79
Vollmer C., Hoppe P., Brenker F. E., 2008, ApJ, 684, 611
Voronin B. A., Tennyson J., Tolchenov R. N., Lugovskoy A. A., Yurchenko S. N., 2010, MNRAS, 402, 492
Zobov N. F., Polyansky O. L., Le Sueur C. R., Tennyson J., 1996, Chem. Phys. Lett., 260, 381
Zobov N. F., Shirin S. V., Polyansky O. L., Tennyson J., Coheur P.-F., Bernath P. F., Carleer M., Colin R., 2005, Chem. Phys. Lett., 414, 193

SUPPORTING INFORMATION

Supplementary data are available at *MNRAS* online.

suppl_data

Please note: Oxford University Press is not responsible for the content or functionality of any supporting materials supplied by the authors. Any queries (other than missing material) should be directed to the corresponding author for the article.

This paper has been typeset from a TEX/LATEX file prepared by the author.